

Stability of the self-phase-locked pump-enhanced singly resonant parametric oscillator

Jean-Jacques Zondy*

BNM-SYRTE (UMR-CNRS 8630), 61 avenue de l'Observatoire, F-75014 Paris, France

(Dated: October 29, 2018)

Steady-state and dynamics of the self-phase-locked ($3\omega \rightarrow 2\omega, \omega$) subharmonic optical parametric oscillator are analyzed in the pump-and-signal resonant configurations, using an approximate analytical model and a full propagation model. The upper branch solutions are found always stable, regardless of the degree of pump enhancement. The domain of existence of stationary states is found to critically depend on the phase-mismatch of the competing second-harmonic process.

PACS numbers: 42.65.Yj, 42.65.Sf, 42.65.Ky

A new class of subharmonic (frequency divide-by-three, or $3 \div 1$) optical parametric oscillators (OPOs), namely *self-phase-locked* (SPL-OPOs), has aroused lately much interest from both the experimental [1, 2] and theoretical [3, 4, 5] standpoints. Consider a $3 \div 1$ OPO pumped at an angular frequency $\omega_p = 3\omega$ (generating signal and idler waves at $\omega_s = 2\omega$ and $\omega_i = \omega$) containing a second nonlinear crystal that is phase-matched for the competing second-harmonic (degenerate down-conversion) of the idler (signal) waves. The loss-free $\chi^{(2)}$ medium of total length $L = L_1 + L_2$ consists of a dual-grating periodically-poled (PP) crystal comprising a first section of length L_1 perfectly phase-matched for the $\chi_{\text{OPO}}^{(2)} \equiv \chi^{(2)}(-3\omega; 2\omega, \omega)$ down-conversion, followed by a second section of length L_2 nearly phase-matched for the competing $\chi_{\text{SHG}}^{(2)} \equiv \chi^{(2)}(-2\omega; \omega, \omega)$ process with a wavevector mismatch $\Delta k = k_{2\omega} - 2k_\omega \neq 0$. Due to the mutual self-injection of the subharmonic waves, the dynamics of the signal-and-idler resonant devices was recently shown to depart from that of a conventional ($L_2 = 0$) non-degenerate OPO [3]. The main difference is that SPL-OPOs are characterized by an intensity bistability (sub-critical bifurcation) whatever the configuration [3, 4, 5]. Secondly, each intensity state of the stable branch can take 3 possible deterministic phase values equally spaced by $2\pi/3$, while conventional OPOs are subject to a stochastic phase diffusion process [6]. Experimentally, $3 \div 1$ SPL-OPOs are investigated in frequency metrology [1, 7, 8], Fourier synthesis of attosecond pulse [2], transverse pattern formation [4, 5] and potentially for new features in squeezed states of light. Finally, owing to the much lower pump intensity requirement, SPL-OPOs should be also suited for the first experimental evidence of a Hopf bifurcation in cw OPOs, predicted to only occur in triply-resonant OPOs under extreme detuning conditions [9].

In this brief report, I provide an analysis of the pump-enhanced singly resonant device (SPL-PRSRO) which was only over-viewed in the conclusion of Ref. [3]. Bearing in mind that PRSROs are easier to implement than

DRO/TROs (subject to mode pair instabilities) or SROs (requirement of high pump thresholds), it is interesting to check how the dynamics of the doubly/triply resonant SPL-OPOs is affected when only one of the subharmonic waves oscillates with a varying pump enhancement, and to compare with the behaviour of the purely idler-resonant (SPL-IRO) case treated by Longhi in the mean-field approximation and neglecting pump depletion [5].

The analysis starts with the solutions of the reduced propagation equations for the normalized slowly varying field envelopes $A_j(t', Z) = g_1 L_1 N_j(t', Z)$ ($j = p, s, i$) throughout the dual-section medium. The complex amplitudes are scaled such that their intensities $I_j = |A_j|^2$ are proportional to the number of photons $|N_j|^2$ in j -th mode, times the square of the small-signal parametric gain $g_1 L_1$ ($\ll 1$) of the $3 \div 1$ process ($g_1 \propto \chi_{\text{OPO}}^{(2)}$) [3]. In the phase-retarded time frame ($t = t' - \bar{n}Z/c$; $z = Z/L_1$ or $z' = Z/L_2$), where \bar{n} is the average index of refraction, the 3 plane-wave equations for $0 \leq z \leq L_1/L_1 = 1$ are

$$\partial_z A_p = iA_i A_s; \quad \partial_z A_{s,i} = iA_p A_{i,s}^*, \quad (1)$$

with the initial condition $A_i(z = 0) = 0$ (non-resonant idler). In the SHG section ($0 \leq z' \leq L_2/L_2 = 1$), the subharmonic amplitudes evolve as

$$\partial_{z'} A_s = iS A_i^2 \exp(+i2\xi z'), \quad (2)$$

$$\partial_{z'} A_i = iS A_s A_i^* \exp(-i2\xi z') \quad (3)$$

with the initial conditions $A_{s,i}(z' = 0) = A_{s,i}(z = 1)$, while the pump amplitude keeps its value at $z = 1$ throughout the second section ($\partial_{z'} A_p = 0$). The parameter $\xi = \Delta k L_2/2$ is the phase mismatch of the competing SHG process. The nonlinear coupling parameter $S = g_2 L_2/g_1 L_1$ is the ratio of the SHG to OPO small signal gains ($g_2 \propto \chi_{\text{SHG}}^{(2)}$). Its expression reduces to $S \simeq (L_2/L_1)/\sqrt{3}$ for a $3 \div 1$ OPO employing a PP material [3]. The time-dependent cavity dynamics is obtained from an iterative mapping of the resonating field amplitudes at $z' = 1$ and at a time t to their values at $z = 0$ after one roundtrip time τ of the ring-type cavity,

$$A_j(t + \tau, z = 0) = r_j \exp(i\Delta_j) A_j(t, z' = 1) + A_{in,j}(4)$$

with $j = p, s$ and with r_j being the (real) amplitude reflectivity from $z' = 1$ back to $z = 0$. The constant input

*Electronic address: jean-jacques.zondy@obspm.fr

field A_{in} stands for the driving pump field and is null for the signal wave. The r_j 's are related to the cavity loss parameters κ_j 's by $\kappa_j = 1 - r_j$. For the resonating subharmonic, it will be always assumed that $\kappa_s \ll 1$, $r_s \simeq 1$. The amplitude loss parameter κ_s is then related to the cavity finesse by $F_s = \pi/\kappa_s$ and to the cavity half linewidth γ_s by $2\pi\gamma_s = \kappa_s/\tau$. The phase factors Δ_j correspond to the linear propagation (and mirror) phase shifts, modulo 2π . The Δ 's, also called cavity detuning parameters, are equal to $(\nu - \nu_c)\tau$, e.g. to the wave frequency mismatches from the nearest cold cavity frequency, scaled to the free spectral range $1/\tau$.

The dynamics of the systems can be numerically studied without any approximation by solving Eqs.(1-3) using a fourth-order Runge-Kutta solver with the appropriate initial conditions and making use of the boundary conditions (4) (*propagation* model). Unstable fixed point cannot be found numerically so that approximate analytic solutions of the steady state equations must be worked out by expanding the amplitudes in Mac Laurin series of z , e.g. $A_j(z) = A_j(0) + \sum_{n=1}^{\infty} [\partial_z^{(n)} A_j]_0 z^n/n!$, which allows to integrate Eqs.(1-3). Such an expansion is justified by the smallness of the scaled amplitudes ($|A_j| \leq 1$) since $g_1 L_1 \ll 1$ and because $z, z' < 1$. The n -th order derivatives can be evaluated in terms of the field products at $z = 0$ using the generic equations (1)-(3). To get the leading(fourth)-order coupling terms from this perturbative approach, only the $n = 1$ terms in the field expansions need to be kept. After some algebra, the approximate solutions of (1)-(3) are

$$A_p(t, L_1 + L_2) = A_p(t, 0) - (1/2)A_p(t, 0) |A_s(t, 0)|^2, \quad (5)$$

$$A_s(t, L_1 + L_2) = A_s(t, 0) + (1/2)A_s(t, 0) |A_p(t, 0)|^2 - i\chi^* A_p^2(t, 0) [A_s^*(t, 0)]^2, \quad (6)$$

$$A_i(t, L_1 + L_2) = iA_p(t, 0)A_s^*(t, 0) + \chi A_p^*(t, 0)A_s^2(t, 0) \quad (7)$$

where the nonlinear coupling parameter is $\chi = S \exp(-i\xi)(\sin \xi/\xi)$. These solutions which assume a linear z -variation of the fields depart from the numerical ones for decreasing pump resonance (SRO limit), but still account for pump depletion to first order. The cubic term in Eq.(5), present in conventional PRSRO model [10], is due to the usual cascading ($3\omega - 2\omega = \omega$) followed by the re-combination process ($\omega + 2\omega = 3\omega$), while the last quartic term in Eq.(6), describing the two-step processes ($3\omega - 2\omega = \omega$) followed by ($\omega + \omega = 2\omega$), leads to injection-locking. Note that this term is quadratic in the signal-and-idler resonant cases (see Eqs.(9) in Ref. [3]) or in the pure IRO case without pump depletion (see Eq.(11) of Ref. [5]). Stationary solutions to Eqs.(4)-(6) are obtained by requiring that $A_{p,s}(t+\tau, 0) = A_{p,s}(t, 0) \equiv A_{p,s}$. Considering small enough detuning ($\Delta_{p,s} \ll 2\pi$), the exponential phase factor in Eq.(4) is expanded as $\sim 1 + i\Delta_j$. The resulting steady state amplitude equations are

$$\begin{aligned} (\kappa_p - ir_p\Delta_p)A_p &= -(1/2)r_p(1 + i\Delta_p)A_p |A_s|^2 + A_{in}, \\ \frac{\kappa_s - i\Delta_s}{r_s(1 + i\Delta_s)}A_s &= [(1/2)A_s A_p]^2 - i\chi^* A_p^2 [A_s^*]^2. \end{aligned} \quad (8)$$

The above Mac-Laurin solutions (as compared with the mean-field approach based on amplitude expansion in the power of the κ 's [5]) converge satisfactorily to the full propagation model as long as $r_p \geq 0.8$. Excellent convergence (to $\pm 3\%$ for the parameters of Fig.3, for instance) is found when both the pump and signal experience low roundtrip loss, not exceeding a few percent even for large pumping ($I_{in} = |A_{in}|^2$ up to ~ 50 times the threshold for oscillation). For decreasing pump resonance and moderate pumping they still provide a qualitative account of the dynamical behavior of the system, although resulting in higher values of the intensities $I_j = |A_j|^2$. The domain of validity of the Mac Laurin model will be shown to depend on the value of r_p . In the true SRO limit ($r_p \rightarrow 0$), the full propagation model remains always valid.

Besides the trivial (non-lasing) solutions $A_{s,i} = 0$, $A_p = A_{in}/(\kappa_p - ir_p\Delta_p)$, Eqs.(8) admit non-zero intensity states $I_{p,s} = |A_{p,s}|^2$ with well-defined phases. It is convenient to introduce the scaled intensities $\bar{I}_p = I_p/I_p^{th}$, $\bar{I}_s = I_s/I_s$, $\bar{I}_i = I_i/(I_p^{th}I_s)$, with $I_p^{th} = 2\kappa_s$, $I_s = 2\kappa_p/r_p$; input pump intensity $\bar{I}_{in} = I_{in}/(2\kappa_p^2\kappa_s)$; and normalized cavity detuning $\bar{\Delta}_{p,s} = \Delta_{p,s}/\kappa_{p,s}$. Introducing $C_s = 4|\chi|^2(\kappa_p/r_p)$, and taking the moduli of (8), the scaled signal intensity \bar{I}_s is then the solution of

$$\begin{aligned} [F(1 - r_s\kappa_s\bar{\Delta}_s^2) - r_s(1 + \kappa_s^2\bar{\Delta}_s^2)\bar{I}_{in}]^2 + (\bar{\Delta}_s F)^2 \\ = 2C_s r_s^2(1 + \kappa_s^2\bar{\Delta}_s^2)^2 \bar{I}_s \bar{I}_{in}^2, \end{aligned} \quad (9)$$

where the symbol F stands for

$$F = (1 + \bar{I}_s)^2 + \bar{\Delta}_p^2(\kappa_p\bar{I}_s - r_p)^2. \quad (10)$$

The intracavity pump is given by $F\bar{I}_p = \bar{I}_{in}$ and the idler intensity by $\bar{I}_i = \bar{I}_p\bar{I}_s[1 + \bar{I}_s|\chi|\bar{I}_s + (\bar{I}_p - 1)/\bar{I}_p]$.

Phase relationships, demonstrating phase-locking of the subharmonic waves to the pump laser, can be derived from Eqs.(8) by writing $A_j = \alpha_j \exp(i\varphi_j)$ where α_j are the amplitude moduli. Defining φ_{in} as the arbitrary phase of the pump laser and $\varphi_D = \xi + 2\varphi_p - 3\varphi_s$, one obtains

$$\tan(\varphi_{in} - \varphi_p) = -[\bar{\Delta}_p(r_p - \kappa_p\bar{I}_s)]/[1 + \bar{I}_s], \quad (11)$$

$$\cot \varphi_D = \bar{\Delta}_s/[1 - r_s\kappa_s\bar{\Delta}_s^2 - r_s(1 + \kappa_s^2\bar{\Delta}_s^2)\bar{I}_p]. \quad (12)$$

When solved for φ_s , these relations yield 3 possible values $\varphi_s = \varphi_0 + 2k\pi/3$ (φ_0 being a constant and $k = 0, \pm 1$), while for $|\chi| = 0$ only the sum phase $\varphi_s + \varphi_i = \varphi_p + \pi/2$ is deterministic as predicted for conventional oscillators, due to the phase diffusion noise stemming from the spontaneous parametric fluorescence [6]. Furthermore, when $|\chi| = 0$ ($C_s = 0$), Eq.(9) implies that the signal resonates necessarily with zero detuning ($\bar{\Delta}_s = 0$), and one retrieves the result that the intracavity pump is clamped to the constant value $\bar{I}_p = 1$ for any \bar{I}_{in} [10]. From Eq.(10), \bar{I}_s is then the solution of a quadratic equation which admits a single positive solution (supercritical bifurcation) if and only if $\bar{I}_{in}(1 + \kappa_p^2\bar{\Delta}_p^2) - \bar{\Delta}_p^2 \geq 0$. This condition is always satisfied for $\bar{I}_{in} \geq \bar{I}_{th}$, where the input (intracavity)

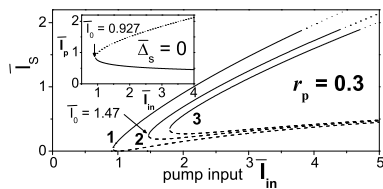


FIG. 1: Bifurcation diagram of signal intensity versus pump parameter, computed from the Mc Laurin solutions, for $r_p = 0.3$, $\Delta_p = 0$, $\kappa_s = 0.005$, $\chi = S = 0.2$. Curves (1)-(3) are for $\bar{\Delta}_s = 0; 0.4; 0.5$. The inset plots show the intracavity pump stable (solid line) and unstable (dashed) fixed points \bar{I}_p^\pm . Note that \bar{I}_s^+ diverges at $\bar{I}_{in} \geq 3.8; 4.4; 4.7$ for curves 1;2;3 from either the LSA analysis or the time mapping of Eqs.(5)-(7), setting the validity range of the Mc Laurin approximation.

pump threshold expresses as $\bar{I}_{th} = 1 + r_p^2 \bar{\Delta}_p^2$. Considering now the case $|\chi| \neq 0$, the signal wave is *a priori* no longer constrained to oscillate with zero detuning and its intensity is the solution of a quartic equation, $\sum_{n=0}^4 a_n \bar{I}_s^n = 0$, obtained by expanding Eq.(9) using Eq.(10). The numerical resolution of this equation for a wide range of signal detuning or driving pump intensity always yield two real positive roots \bar{I}_s^\pm , defining two branches of solutions, for pump intensities $\bar{I}_{in} \geq \bar{I}_0$ (see below for definition of \bar{I}_0). The stability of these two fixed points, each associated with the 3 possible phase states, was investigated using a linear stability analysis (LSA) [3] that leads to a quartic characteristic equation, $\sum_{n=0}^4 \Phi_n \Lambda^n = 0$. The LSA results were double-checked by a direct time mapping of Eqs.(5)-(6) using the boundary conditions (4). From the LSA of the trivial state, the threshold for oscillation (not necessarily on a stable fixed point) remains the same as for conventional devices. Fig.1 shows the analytical bifurcation plot versus the pump parameter for $r_p = 0.3$ and 3 different values for $\bar{\Delta}_s$, as compared with the solutions computed with the propagation model (Fig.2). The bifurcation diagram versus \bar{I}_{in} displays a saddle-node region, with \bar{I}_0 being the input intensity at the saddle-node point where $\bar{I}_s^+ = \bar{I}_s^-$. For zero or vanishingly small $\bar{\Delta}_s$, one has $\bar{I}_0 < \bar{I}_{th}$ but as the detuning is increased, $\bar{I}_0 > \bar{I}_{th}$. This behavior contrasts with the signal-and-idler resonant cases, for which a transition from sub-criticality to super-criticality is predicted when $\bar{\Delta}_{s,i} \rightarrow 0$, corresponding to the merging of the saddle-node point of coordinate $(\bar{I}_0, \bar{I}_s \neq 0)$ with the threshold point $(\bar{I}_{th}, \bar{I}_s = 0)$ [3]. Note also the tiny range of sub-threshold states in curve (1), resulting from the weak self-injection regime. From the LSA of the Mc Laurin solutions, the \bar{I}_s^- branches (dashed curves) are always unstable, due to a positive real eigenvalue, but only a portion of the upper branch (solid lines) extending from the saddle-node intensity \bar{I}_0 to some critical intensity \bar{I}_C is found stable. The instability (dotted lines) beyond \bar{I}_C (characterized by 3 real positive eigenvalues of the LSA equation) was confirmed by the time mapping of the Mc Laurin solutions which diverges at \bar{I}_C , whereas the

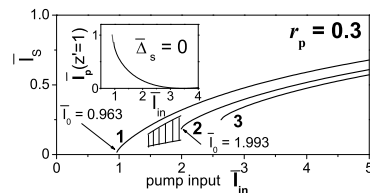


FIG. 2: Stable (upper) branches of signal intensity versus pump parameter, computed from the propagation model with the same parameters as for Fig.1. The hatched domain at the left of curve (2) gives the amplitude of the limit cycles below the saddle-node intensity \bar{I}_0 (non-stationary SPL states). The inset plots show the output ($z' = 1$) intracavity pump \bar{I}_p .

full propagation model converge to a fixed point for any input intensity value (Fig. 2). Hence the whole upper branch of the SPL-PRSRO is actually stable, the instability predicted by the Mc Laurin model being merely an artefact of the approximation. Actually, as the pump enhancement is decreased the validity range of the Mc Laurin model is restricted to pump parameters lying closer and closer to the threshold. In Fig. 2, obtained by backward adiabatic following of the stationary solutions, all curves end at their saddle-node point \bar{I}_0 since critical slowing down is observed as these points are approached. The limit cycles occurring for $\bar{I}_{in} < \bar{I}_0$ (hatched area) are merely due to the non-existence of stationary states. The upper branch is found stable even in the SRO limit ($r_p = 0$), whatever the detunings, in contrast with the SPL-IRO mean-field analysis results [5]. Let us remind that in the SPL-DRO/TROs the upper branch was found to destabilize via a Hopf bifurcation [3]. The difference in dynamical behavior is due to the stronger self-injection regime in these latter devices. The inset frame in Fig. 2 gives the output pump intensity (at $z' = 1$) corresponding to $\bar{\Delta}_{p,s} = 0$ (curve (1)), it can be seen that the pump is no longer clamped to unity as in conventional PRSROs [10], meaning that the competing nonlinearity enhances the down-conversion efficiency. In Fig. 3, as

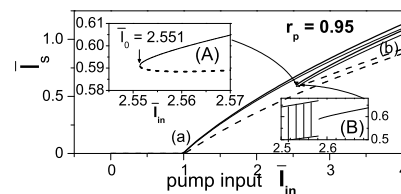


FIG. 3: Bifurcation diagram of signal intensity versus pump parameter, computed from the analytical model for $r_p = 0.95$ and same other parameters as in Fig.1, excepted that curves (a)-(b) are for $\bar{\Delta}_s = 0; 0.1$. The thin solid lines under-riding the (a)-(b) solid lines show the upper branch computed from the propagation model. The insets (A: Mc Laurin model, B: propagation model) are blow-ups of the saddle-node region of (a) case. In (B), critical slowing-down characteristic of saddle-node points occurs.

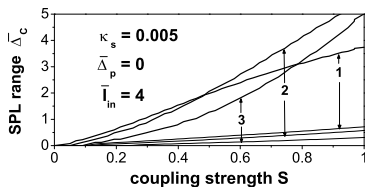


FIG. 4: Critical values of the signal detuning parameter delimiting the boundary of stable (underneath the curves) and oscillatory SPL states (above) in the $(\bar{\Delta}_s, S)$ plane at fixed pump input/detuning, computed from the propagation model. The thick solid lines are for $r_p = 0.3$ and the thin lines for $r_p = 0.95$. The curve labels (1)-(3) stand for $\xi = 0, \pi/2, 3\pi/4$.

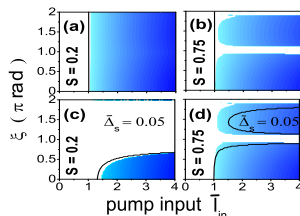


FIG. 5: Domain of stability (dark region) of phase-locked states in the (ξ, \bar{I}_{in}) plane (propagation model), with $r_p = 0.95$, $\kappa_s = 0.005$, $\bar{\Delta}_p = 0$: (a),(c) for $S = 0.2$ and (b),(d) for $S = 0.75$. Upper (lower) frames are for $\bar{\Delta}_s = 0$ ($\bar{\Delta}_s = 0.05$). The solid lines give the boundary of existence of stationary states from the Mc Laurin model. The plots are symmetric for negative phase mismatch ξ .

the pump finesse increases ($\kappa_p = 0.05$), the Mc-Laurin (thick solid lines) and the propagation model (thin solid lines) converge excellently for any input intensity. Both models predict then a whole upper branch stability, for a wide range of input intensity (up to tested $\bar{I}_{in} = 50$ at least). The Mc Laurin model converges to the propagation model because when $\kappa_p \rightarrow 0$ the assumption of a linear z -dependence of the resonating fields inside the medium is fully justified (uniform field limit). Notice that the threshold value is then more sensitive to the signal detuning than in Fig. 2. As a consequence of the reduced sub-threshold state range due to the weak SPL regime one expect that the self-locking detuning range,

defined as the maximum allowed $\bar{\Delta}_s$ for a given pump input intensity, would be smaller than in signal-and-idler resonant set-ups. Indeed large pump enhancement is paid back with a shrinking self-locking range. Fig.4 displays the critical $\bar{\Delta}_C(S)$ detuning for both $r_p = 0.3$ and $r_p = 0.95$, when $\bar{\Delta}_p = 0$ and when the device is pumped 4 times above threshold. Surprisingly, for the same non-linear coupling strength S , the high pump resonance case leads to less than a cavity linewidth SPL range, while for the SRO limiting case the SPL range is 10-fold wider, as with SPL-DRO/TROs. Hence a large SPL range is not necessarily associated with the double-resonance condition that involves a strong mutual-injection process between the subharmonics. The small (< 1 -MHz, e.g. less than a cavity linewidth) self-locking range reported by Boller *et al* [1] for a SPL-PRSRO is in agreement with this expectation. As a noticeable difference with the signal-and-idler resonant cases, the coefficients of the LSA equation depend on the phase of the coupling parameter χ , while χ enters only as its modulus in the SPL-DRO stability analysis (see the Appendix in Ref.[3]). One hence expects that the dynamics of SPL-PRSROs will be sensitive to the SHG phase mismatch ξ . Fig.5 shows the steady-state signal intensity contour plots in the parameter space (\bar{I}_{in}, ξ) , computed with the propagation model for $\bar{I}_{in} = 4$, $r_p = 0.95$, $\bar{\Delta}_p = 0$ and two values $S = 0.2$ (a,c) and $S = 0.75$ (b,d) of the coupling parameter. For the stronger coupling $S = 0.75$ (panels b-d), small amplitude limit cycles arise around $\xi = \pm\pi$, even for $\bar{\delta}_s = 0$ (panel b). To avoid such non-stationary states, it is important to tailor accurately the simultaneous phase-matching of both competing processes.

In conclusion, it is found that the whole upper branch of the SPL-(PR)SRO is stable and that the self-locking range shrinks with increasing pump enhancement. In the SRO limit, the approximated model may fail to describe correctly the dynamical behavior over a large pump input range. Of more concern, in contrast with signal-and-idler resonant devices, the domain of existence of stationary phase-locked states is found sensitive to the value of the residual phase mismatch of the competing SHG nonlinearity. The author is indebted to one of the referees for his personal involvement in the improvement of this report. This work has benefited from a partial support from an European Union INCO-Copernicus grant (Contract No. ERBIC15CT980814).

[1] K. Boller *et al*, Opt. Expr. **5**, 114 (1999).
[2] Y. Kobayashi, K. Torizuka, Opt. Lett. **25**, 856 (2000).
[3] J.-J. Zondy *et al*, Phys. Rev. A **63**, 023814 (2001).
[4] S. Longhi, Phys. Rev. E **63**, 055202(R) (2001).
[5] S. Longhi, Eur. Phys. J.D **17**, 57 (2001).
[6] R. Graham, H. Haken, Zeit. für Phys. **210**, 276 (1968).

[7] A. Douillet *et al*, IEEE Trans. Instr. Meas. **50**, 548 (2001).
[8] S. Slyusarev *et al*, Opt. Lett. **24**, 1856 (1999).
[9] L. A. Lugiato *et al*, Il Nuovo Cimento **10D**, 959 (1988).
[10] S. Schiller *et al*, J. Opt. Soc. Am. B **16**, 1512-1524 (1999).